NONLINEAR H_∞ HELICOPTER HOVERING CONTROL AND IMPLEMENTATION USING CSIA

Chien-Chung Kung[1], Ciann-Dong Yang[2]

National Defense University[1]
Chung Cheng Institute of Technology
Tao-Yuan 335, Taiwan
Tel:886-3-3906751
Fax:886-3-3906419
Email: cckung@ccit.edu.tw

National Cheng Kung University[2]
Institute of Aeronautics and Astronautics
Tainan 701, Taiwan
Tel : 886-6-2757575 ext. 63669
Fax : 886-6-2389940
E-mail: cdyang@mail.ncku.edu.tw

Keywords: Nonlinear H_∞ Control; Helicopter Hovering Control; Control Surface Inverse Algorithm (CSIA); Separation Principle of Nonlinar H_∞Hovering Control.

Abstract

This paper applies the nonlinear H_∞ control theory to helicopter hovering manuver whose complete six degree-of-freedom nonlinear equations of motion with coupled rotor and inflow dynamics are considered directly without linearization. Under this approach, the exact nonlinear equations governing both the longitudinal and lateral motions are considered. The control surface inverse algorithm (CSIA) developed in this paper to implement the nonlinear H_∞ control surface deflections is based on Moore-Penrose generalized inverse. The implement technique is constructed based on minimizing the global errors between the nonlinear H_∞ commands and actual control forces and moments. The separation principle of nonlinear H_∞ hovering control is verified by CSIA under actuator with saturation and rate limit.

Nomenclature

R	rotor radius (subscript T denotes tail rotor) (m)
ρ	air density (kg/m^3)
Ω	main rotor speed (subscript T denotes tail rotor) (rad/s)
β_0 ,β_{1c}, β_{1s}	collective, longitudinal and lateral flapping angle of rotor blade (subscript w denotes hub/wind axes) – in multi-blade coordinates (rad)
θ_{1c}, θ_{1s}	longitudinal and lateral cyclic pitch (subscript w denotes hub/wind axes) (rad)
C_T, C_{T_T}	main rotor and tail rotor thrust coefficients
γ_s	shaft angle(positive forward, rad)
Ψ_w	rotor sideslip angle (rad)
$F_{1s}^{(1)}$	one-per-rev sine component of out-of-plane rotor balde force
$F_{2s}^{(1)}$	two-per-rev sine component of out-of-plane rotor balde force
$F_{2c}^{(1)}$	two-per-rev cosine component of out-of-plane rotor balde force
$F_{1s}^{(2)}$	one-per-rev sine component of in-plane rotor balde force
$F_{1c}^{(2)}$	one-per-rev cosine component of in-plane rotor balde force
β_{1cwT}	tail rotor cyclic flapping angle in tail rotor hub /wind axes (rad)
a_0 , a_{0_T}	main rotor and tail rotor blade lift curve slopes (1/rad)
μ_f	nodimensional total velocity incident on fuselage
$\overline{S}_p$	nodimensional fuselage plane area
C_{xf}	normalized fuselage x-axis force coefficient
θ	pitch angle
μ	normalized velocity in x-axis in hub-wind axis system
μ_T	normalized velocity at tail rotor
μ_{z_T}	total normalized tail rotor inflow velocity
θ_0,θ_{0T}	main and tail rotor collective pitch angles (rad)
s, s_T	solidities of main rotor and tail rotor
θ_{1s}	Longitudinal cyclic pitch (subscript hw denotes hub/wind axes)(rad)
λ_0, λ_{0T}	main rotor and tail rotor uniform inflow velocities in hub/shaft axes (normalized by ΩR)
θ_{tw}	main rotor blade linear twist (rad)
c	rotor blade chord (m)
I_β	flap moment of inertia (kg-m^2)
K_β	Center-spring rotor stiffness (N-m/rad)
δ_3, k_3	mechanical hinge set angle (rad), k_3=tanδ_3
γ_n , γ_T	Lock numbers of main rotor and tail rotor
λ_{β_T}	tail rotor flap frequency ratio
γ_{1s}	rotor first harmonic longitudinal inflow velocity in hub/shaft axes (subscript hw denotes hub/wind axes) (normalized by ΩR)

1 Introduction

Many studies were established for dynamics of helicopter. Padfield [1] has summarized the modeling of a helicopter, and discussed about helicopter flying qualities. Based on Padfield's results, we built our helicopter model. Several references can be found that use robust control techniques for helicopter hover-control design, e.g. Apkarian et al [2]. The practical application of nonlinear H_∞ control theory is limited due to the difficulties in solving the associated Hamilton-Jacobi partial differential inequality (HJPDI). Recently, nonlinear H_∞ control has been applied to nonlinear spacecraft [3], flight control [4]. The paper here derived control surface inverse algorithm (CSIA) to implement nonlinear H_∞

helicopter hovering control, which has not been considered in the literature before.

2 Explicit Aerodynamic Model

A helicopter can be modeled as the combination of five interacting sub-systems: mainrotor, fuselage, empennage, tailrotor and engine[1]. The six degree-of-freedom rigid body motion of helicopter can be described as following:

$$m_S\dot{U} = m_S\left(-WQ+VR\right)+F_x+d_x \quad (1a)$$

$$m_S\dot{V} = m_S\left(-UR+WP\right)+F_y+d_y \quad (1b)$$

$$m_S\dot{W} = m_S\left(-VP+UQ\right)+F_z+d_z \quad (1c)$$

$$I_{xx}\dot{P}=I_{xz}\left(\dot{R}+PQ\right)+I_{xy}\left(\dot{Q}-PR\right)-I_{yz}\left(R^2-Q^2\right)+\left(I_{yy}-I_{zz}\right)QR+L+d_l \quad (1d)$$

$$I_{yy}\dot{Q}=I_{xy}\left(\dot{P}+QR\right)+I_{zy}\left(\dot{R}-PQ\right)-I_{xz}\left(P^2-R^2\right)+\left(I_{zz}-I_{xx}\right)PR+M+d_m \quad (1e)$$

$$I_{zz}\dot{R}=I_{yz}\left(\dot{Q}+PR\right)+I_{xz}\left(\dot{P}-QR\right)-I_{yx}\left(Q^2-P^2\right)+\left(I_{xx}-I_{yy}\right)PQ+N+d_n \quad (1f)$$

where U, V, W, and P, Q, R are standard notations for linear and angular velocities, respectively, and all referred to the fuselage (body-fixed) axes system, I_{xx}, I_{xz} , …, etc, are the moments of inertia of the helicopter; m_s is the helicopter's mass. Forces (F_x, F_y, F_z) and moments (L, M, N) consist of (a) aerodynamics force and moment, (b) gravitational force, (c) propulsive force and moment. They can be described as the sum of the contributions from the five sub-systems

$$F_x = X_R+X_T+X_F+X_{tp}+X_{fn}-m_sg\sin\theta \quad (2a)$$

$$F_y = Y_R+Y_T+Y_F+Y_{tp}+Y_{fn}+m_sg\sin\phi\cos\theta \quad (2b)$$

$$F_z = Z_R+Z_T+Z_F+Z_{tp}+Z_{fn}+m_sg\cos\phi\cos\theta \quad (2c)$$

$$L = L_R+L_T+L_F+L_{tp}+L_{fn} \quad (2d)$$

$$M = M_R+M_T+M_F+M_{tp}+M_{fn} \quad (2e)$$

$$N = N_R+N_T+N_F+N_{tp}+N_{fn} \quad (2f)$$

where the subscripts stand for: rotor (R), tail rotor (T), fuselage (F), horizontal tail plane (tp), and vertical fin (fn). The orientation of fuselage is defined in terms of Euler Angle θ and ϕ with respect to an earth-fixed axes system. In the following, each term in the right-hand-side of Eqs.(2) will be expressed as an explicit function of the control variables used in the nonlinear H_∞ approach. To further simplify the notations, the following definitions are used:

$$\Sigma(t)=[U\quad V\quad W]^T=[U_0\quad V_0\quad W_0]^T+[u\quad v\quad w]^T=\Sigma_0+\sigma(t)$$

$$\Omega(t)=[P\quad Q\quad R]^T=[P_0\quad Q_0\quad R_0]^T+[p\quad q\quad r]^T=\Omega_0+\omega(t)$$

$$u_\Sigma(t)=[F_x\quad F_y\quad F_z]^T=[F_{x0}\quad F_{y0}\quad F_{z0}]^T+[f_x\quad f_y\quad f_z]^T=u_{\Sigma_0}+u_\sigma(t)$$

$$u_\Omega(t)=[L\quad M\quad N]^T=[L_0\quad M_0\quad N_0]^T+[l\quad m\quad n]^T=u_{\Omega_0}+u_\omega(t)$$

$$d_\sigma=[d_x\quad d_y\quad d_z]^T,\ d_\omega=[d_l\quad d_m\quad d_n]^T$$

where the symbol with subscript zero denotes the value at equilibrium point (trim condition), and the lower-case symbol denotes the deviation from the equilibrium point. However, it needs to be noted here that we do not make the assumption of small deviation, i.e., the nonlinear terms such as $\sigma^T\sigma$ and $\omega^T\omega$ are not negligible when compared with the linear terms σ and ω. The moments of inertia matrix I_M and the cross-product matrix S(ω) induced by the vector ω=[p q r]^T are defined as

$$I_M=\begin{bmatrix} I_{xx} & -I_{xy} & -I_{xz}\\ -I_{xy} & I_{yy} & -I_{yz}\\ -I_{xz} & -I_{yz} & I_{zz}\end{bmatrix},\ \mathrm{S}(\omega)=\begin{bmatrix} 0 & -r & q\\ r & 0 & -p\\ -q & p & 0\end{bmatrix}$$

The trim force $u_{\Sigma 0}$ and trim moment $u_{\Omega 0}$ can be solved from Eqs.(1) by $\sigma=\dot{\sigma}=\omega=\dot{\omega}=d_\sigma=d_\omega=0$. Substituting $u_{\Sigma 0}$ and $u_{\Omega 0}$ into Eqs.(1), yields the nonlinear equations of motion with respect to the equilibrium point as

$$\dot{\sigma}=-S(\omega)\sigma-S(\Omega_0)\sigma-S(\omega)\Sigma_0+m_s^{-1}u_\sigma+m_s^{-1}d_\sigma \quad (3a)$$

$$\dot{\omega}=-I_M^{-1}S(\omega)I_M\omega-I_M^{-1}S(\omega)I_M\Omega_0-I_M^{-1}S(\Omega_0)I_M\omega+I_M^{-1}u_\omega+I_M^{-1}d_\omega \quad (3b)$$

According to the values of Σ_0 and Ω_0, three helicopter control modes can be defined: (1) Velocity and Body-Rate Control Mode: $\Sigma_0\neq 0$ and $\Omega_0\neq 0$; (2) Velocity and Attitude Control Mode: $\Sigma_0\neq 0$ and $\Omega_0=0$; (3) Hovering Mode: $\Sigma_0=\Omega_0=0$. Letting $\Sigma_0=\Omega_0=0$ in Eqs.(3), we have

$$\frac{d}{dt}\begin{bmatrix}\sigma\\ \omega\end{bmatrix}=\begin{bmatrix}-S(\omega) & 0\\ 0 & -I_M^{-1}S(\omega)I_M\end{bmatrix}\begin{bmatrix}\sigma\\ \omega\end{bmatrix}+\begin{bmatrix}m_s^{-1}I_3 & 0\\ 0 & I_M^{-1}\end{bmatrix}\begin{bmatrix}d_\sigma\\ d_\omega\end{bmatrix}+\begin{bmatrix}m_s^{-1}I_3 & 0\\ 0 & I_M^{-1}\end{bmatrix}\begin{bmatrix}u_\sigma\\ u_\omega\end{bmatrix} \quad (4)$$

It can be seen that, even for hovering mode, the equations of motion are inherently nonlinear. The associated flight control problem is to design the control force u_σ and the control moment u_ω so as to nullify the velocity and body rate of the helicopter and at the same time to track the attitude command $\begin{bmatrix}\phi_0 & \theta_0 & \psi_0\end{bmatrix}$ in the presence of the external disturbance. Eq.(4) can all be recast into the following standard state-space form:

$$\dot{x}=f(x)+g_1(x)d+g_2(x)u \quad (5)$$

where $u=[u_\sigma^T\quad u_\omega^T]^T$ is the nonlinear H_∞ command of control force and moment to be determined in the next section.

3 Nonlinear H_∞ Hovering Control

We will show that under nonlinear H_∞ control structure, the hovering attitude control can be separated from the hovering velocity control. First, we consider Hovering Attitude Control Loop. We need incorporating the quaternion parameters $(\varepsilon_1,\varepsilon_2,\varepsilon_3,\eta)$ to describe the attitude dynamics of the flight vehicle. Applying the representation of quaternion variation as a function of helicopter angular rates, and removing the velocity dynamics from the six degree-of- freedom equations of motion, Eq.(3b) yields

$$\frac{d}{dt}\begin{bmatrix}\varepsilon\\ \eta\\ \omega\end{bmatrix}=\begin{bmatrix}\frac{1}{2}(\eta I+S(\varepsilon))\omega\\ -\frac{1}{2}\varepsilon^T\omega\\ -I_M^{-1}S(\omega)I_M\omega\end{bmatrix}+\begin{bmatrix}0\\0\\I_M^{-1}\end{bmatrix}d_\omega+\begin{bmatrix}0\\0\\I_M^{-1}\end{bmatrix}u_\omega^c=f(x)+g_1(x)d_\omega+g_2(x)u_\omega^c \quad (6)$$

$$z=\begin{bmatrix}\left(\frac{1}{2}\rho_\omega\omega^TI_M\omega+\rho_\eta D^2(\Pi,I_3)\right)^{\frac{1}{2}}\\ \rho_u u_\omega^c\end{bmatrix}=\begin{bmatrix}h_1\\ \rho_u u_\omega^c\end{bmatrix},\ D(\Pi,I_3)=2Cos^{-1}|\eta| \quad (7)$$

where Π is the rotation matrix from the body axes (fuselage coordinate system) to the inertial axes. For notational convenience, let the inertial axes be defined as the desired orientations of the body axes, i.e., let the target value of Π be

I_3. The geodesic metric $D(\Pi, I_3)$ measures the distance between Π and the identity matrix I_3. The main purpose of this control mode is to find u_ω^c such that the system's L_2-gain $\|z\|_{L_2} / \|d_\omega\|_{L_2} < \gamma$ and keep $D(\Pi, I_3)$ as small as possible, i.e., to keep the perturbed body frame close to the inertial reference frame under the action of exogenous disturbance. It can be shown (see Ref. [5]) that $\|z\|_{L_2} / \|d_\omega\|_{L_2} < \gamma$ is achieved if there exists a scalar C^1 function E: $R^n \to R^+$ with E(0)=0, satisfying the following HJPDI

$$\left(\frac{\partial E}{\partial x}\right)^T f + \frac{1}{2}\left(\frac{\partial E}{\partial x}\right)^T \left(\frac{1}{\gamma^2} g_1 g_1^T - g_2 W_E^{-2} g_2^T\right)\left(\frac{\partial E}{\partial x}\right) + \frac{1}{2} h_1^T h_1 < 0 \quad (8)$$

where $\partial E / \partial x = \left[\partial E / \partial x_1 \quad \partial E / \partial x_2 \quad \cdots \quad \partial E / \partial x_n\right]^T$. $W_E = diag(w_x \; w_y \; w_z \; w_l \; w_m \; w_n)$ and ρ_u, ρ_ω, ρ_η in Eqs.(7)~(8) are weighting coefficients concerning the trade-off between tracking performance and control effort. By choosing weighting coefficients properly, it is possible to obtain an acceptably small h_1 without consuming a lot of control effort u_ω^c. If such a qualified E can be found, the nonlinear H_∞ flight controller is then given as

$$u_\omega^c = -W_\omega^{-2} g_2^T \frac{\partial E}{\partial x} \quad (9)$$

Substituting the corresponding $f(x)$, $g_1(x)$, $g_2(x)$, and $h_1(x)$ from Eqs.(6)~(7) into Eq.(8). Motivated from the linear result, we search for a possible quadratic solution in the form

$$E(x) = \frac{1}{2} C_\omega \omega^T I_M \omega + C_{\omega\varepsilon} \omega^T I_M \varepsilon + 2C_\eta (1-\eta) > 0 \quad (10)$$

u_ω^c is determined by Eq.(9) and the result is

$$u_\omega^c = -\frac{1}{\rho_u^2}\left(C_\omega \omega + C_{\omega\varepsilon} \varepsilon\right) \quad (11)$$

Where C_ω and $C_{\omega\varepsilon}$ satisfy

$$C_{\omega\varepsilon} > \sqrt{\frac{\rho_\eta \pi^2 \rho_u^2 \gamma^2}{\gamma^2 - \rho_u^2}}, \; C_\omega > \sqrt{\frac{\rho_u^2 \gamma^2}{\gamma^2 - \rho_u^2}\left[(3C_{\omega\varepsilon} + \rho_\omega / 2)\|I_M\|\right]} \quad (12)$$

Next, we consider Hovering Velocity Control Loop. From Eq.(3a), the hovering velocity dynamics is given by

$$\dot{\sigma} = -S(\omega)\sigma + \frac{1}{m_s} d_\sigma + \frac{1}{m_s} u_\sigma = f(x) + g_1(x) d_\sigma + g_2(x) u_\sigma^c \quad (13)$$

$$z = \begin{bmatrix} \left(\frac{1}{2}\rho_\sigma m_s \sigma^T \sigma\right)^{\frac{1}{2}} \\ \rho_u u_\sigma \end{bmatrix} = \begin{bmatrix} h_1 \\ \rho_u u_\sigma \end{bmatrix} \quad (14)$$

And the corresponding control problem is to determine u_σ^c such that the system's L_2-gain $\|z\|_{L_2} / \|d_\sigma\|_{L_2} < \gamma$. The candidate solution of the HJPDI is chosen as

$$E(x) = \frac{1}{2} C_\sigma m_s \sigma^T \sigma \quad (15)$$

At the first glance, the velocity dynamics interacts with the attitude dynamics via the term $S(\omega)$ in Eq.(13); however, the interacting term during the formation of HJPDI with states $x=\sigma$ in Eq. (8) disappears by means of the property:

$$\left(\frac{\partial E}{\partial \sigma}\right)^T f = C_\sigma m_s \sigma^T \left(-S(\omega)\sigma\right) = 0$$

Which makes the final hovering velocity controller u_σ *independent* of u_ω:

$$u_\sigma = -\frac{1}{\rho_u^2} C_\sigma \sigma, \quad C_\sigma \geq \sqrt{\frac{m_s \rho_\sigma \rho_u^2 \gamma^2}{2(\gamma^2 - \rho_u^2)}} \quad (16)$$

The result means that the six degree-of-freedom hovering control design can be divided into two independent loops: the velocity control loop wherein only velocity dynamics is considered, and the attitude control loop wherein only attitude dynamics is considered. It is so-called nonlinear $H\infty$ hovering control separation principle.

4 Helicopter Pitch Control

The desired forces and moments commands u^c of a helicopter to withstand the exogenous disturbances have been obtained in Eq.(11) and Eq.(16) by nonlinear H_∞ control theory. For a typical helicopter with four pitch control [1], it is not possible to exactly implement the nonlinear H_∞ command u^c, which has six independent components. The best forces and moments u^b which can be generated by helicopter pitch control to follow the command u^c is determined such that the following command tracking error is minimized:

$$J_{error} = \left(Q_u u^c - u^b\right)^T \left(Q_u u^c - u^b\right) \quad (17)$$

where weighting matrix Q_u is used to filter the force and moment commands u^c in order that the pitch control actuators can be operated in their unsaturated regions. Usually we can express u^b (including forces and moments, coming from the various helicopter components) explicitly in terms of blade pitch angles $(\theta_0, \theta_{1c}, \theta_{1s}, \theta_{0_T})$, flapping angles $(\beta_0, \beta_{1c}, \beta_{1s})$, and thrust coefficients (C_T, C_{T_r}). In general, only four of these parameters are independent; once any four of these parameters are given, the remaining parameters are determined accordingly. Careful inspection of the explicit model[1] indicates that the forces and moments can be most naturally expressed in terms of the four parameters: β_{1c}, β_{1s}, C_T, and C_{T_r}. We will start with x-axis total force F_x in Eq.(2 a).

$$\overline{F}_x = \overline{F}_{x_c} + \overline{F}_{x_{C_T}} C_T + \overline{F}_{x_{\beta_{1c}}} \beta_{1c} + \overline{F}_{x_{\beta_{1s}}} \beta_{1s} + \overline{F}_{x_{C_{T_T}}} C_{T_T} \quad (18)$$

where $\overline{F}_x = F_x / (\rho\pi\Omega^2 R^4)$, and

$$\begin{aligned}
\overline{F}_{x_{C_T}} &= (\beta_{1cw} \cos\psi_w \cos\gamma_s + \beta_{1sw} \sin\psi_w \cos\gamma_s + 2\sin\gamma_s)/2 \\
\overline{F}_{x_{\beta_{1c}}} &= a_0 s(\cos\gamma_s)(F_{2c}^{(1)} \cos 2\psi_w + F_{2s}^{(1)} \sin 2\psi_w)/8 \\
\overline{F}_{x_{\beta_{1s}}} &= a_0 s(\cos\gamma_s)(-F_{2c}^{(1)} \sin 2\psi_w + F_{2s}^{(1)} \cos 2\psi_w)/8 \\
\overline{F}_{x_{C_{T_T}}} &= \nu_T \beta_{1cwT}, \quad \nu_T = (\Omega_T / \Omega)^2 (R_T / R)^4 \\
\overline{F}_{x_c} &= a_0 s(\cos\gamma_s)(F_{1c}^{(1)} \beta_0 \cos\psi_w + F_{1s}^{(2)} \cos\psi_w + F_{1s}^{(1)} \beta_0 \sin\psi_w \\
&\quad - F_{1c}^{(2)} \sin\psi_w)/4 + (\mu_f^2/2)\overline{S}_p C_{x_f} - mg\sin\theta/(\rho\pi\Omega^2 R^4)
\end{aligned} \quad (19)$$

The entity with over-bar symbol is non-dimensionalized by the following rules: force is divided by $\rho\pi\Omega^2 R^4$; moment is divided by $\rho\pi\Omega^2 R^5$, area is divided R^2; length is divided by R; velocity is divided by $R\Omega$; angular rate is divided by Ω. The derivations of $\overline{F}_y$, $\overline{F}_z$, $\overline{L}$, $\overline{M}$ and $\overline{N}$ are similar to $\overline{F}_x$. We represent forces $(\overline{F}_x, \overline{F}_y, \overline{F}_z)$ and moments $(\overline{L}, \overline{M}, \overline{N})$ in the form of

$$u^b = A\delta + u^* \tag{20}$$

where

$$u^b = \begin{bmatrix} \bar{F}_x \\ \bar{F}_y \\ \bar{F}_z \\ \bar{L} \\ \bar{M} \\ \bar{N} \end{bmatrix}, \quad A = \begin{bmatrix} \bar{F}_{x_{C_T}} & \bar{F}_{x_{\beta_{1c}}} & \bar{F}_{x_{\beta_{1s}}} & \bar{F}_{x_{C_{T_T}}} \\ \bar{F}_{x_{C_T}} & \bar{F}_{y_{\beta_{1c}}} & \bar{F}_{y_{\beta_{1s}}} & \bar{F}_{y_{C_{T_T}}} \\ \bar{F}_{x_{C_T}} & \bar{F}_{z_{\beta_{1c}}} & \bar{F}_{z_{\beta_{1s}}} & \bar{F}_{z_{C_{T_T}}} \\ \bar{L}_{C_T} & \bar{L}_{\beta_{1c}} & \bar{L}_{\beta_{1s}} & \bar{L}_{C_{T_T}} \\ \bar{M}_{C_T} & \bar{M}_{\beta_{1c}} & \bar{M}_{\beta_{1s}} & \bar{M}_{C_{T_T}} \\ \bar{N}_{C_T} & \bar{N}_{\beta_{1c}} & \bar{N}_{\beta_{1s}} & \bar{N}_{C_{T_T}} \end{bmatrix}, \quad \delta = \begin{bmatrix} C_T \\ \beta_{1c} \\ \beta_{1s} \\ C_{T_T} \end{bmatrix}, \quad u^* = \begin{bmatrix} \bar{X}_c \\ \bar{Y}_c \\ \bar{Z}_c \\ \bar{L}_c \\ \bar{M}_c \\ \bar{N}_c \end{bmatrix}$$

Applying Moore Penrose inverse formula, we can solve the optimal δ minimizing J_{error} as

$$\delta^+ = \left(A^T A\right)^{-1} A^T \left(Q_u u^c - u^*\right) \tag{21}$$

It is noticed that entry of A also depends on the flapping angles and pitch angles that cannot be known in advance. Therefore, an initial guess of δ and an iteration algorithm to obtain the steady-state δ are necessary. The procedures of implementing helicopter pitch control from the nonlinear H_∞ command comprise

(a) Choose an initial guess of θ_0, β_{1c}, β_{1s}, and θ_{0T} to form vector δ.

(b) To iterate the main-rotor inflow .

(c) Search fuselage aerodynamic coefficients:
$C_{y_{fin}}$, $C_{z_{tp}}$, C_{x_f}, C_{y_f}, C_{z_f}, C_{l_f}, C_{m_f}, and C_{n_f} from aero-data table.

(d) To iterate the tail-rotor inflow.

(e) Evaluate Jacobean matrix A and u^* in Eq.(20).

(f) Apply Eq. (21) to solve $\delta^+ = \left[C_T^+ \quad \beta_{1c}^+ \quad \beta_{1s}^+ \quad C_{T_T}^+\right]^T$.

(g) Use C_T^+ to calculate θ_0^+ as

$$\theta_0^+ = \frac{1}{1/3 + \mu^2/2} \begin{bmatrix} \dfrac{2C_T^+}{a_0 s} - \dfrac{\mu}{2}\left(\theta_{1s_{tw}} + \dfrac{\bar{p}_{hw}}{2}\right) \\ -\left(\dfrac{\mu_z - \lambda_0}{2}\right) - \left(\dfrac{1+\mu^2}{4}\right)\theta_{tw} \end{bmatrix} \tag{22}$$

(h) Use θ_0^+ to calculate β_0^+ as

$$\beta_0^+ = \frac{\gamma}{8\lambda_\beta^2} \begin{bmatrix} \theta_0^+\left(1+\mu^2\right) + 4\theta_{tw}\left(\dfrac{1}{5} + \dfrac{\mu^2}{6}\right) + \dfrac{4}{3}\mu\theta_{1s_{tw}} \\ +\dfrac{4}{3}\left(\mu_z - \lambda_0\right) + \dfrac{2}{3}\mu\left(\bar{p}_{hw} - \lambda_{1s_{tw}}\right) \end{bmatrix} \tag{23}$$

(i) Evaluate main-rotor pitch

$$\begin{bmatrix} \theta_0^+ \\ \theta_{1c_w}^+ \\ \theta_{1s_w}^+ \end{bmatrix} = M_\theta^{-1}\left(M_\beta \begin{bmatrix} \beta_0^+ \\ \beta_{1c_w}^+ \\ \beta_{1s_w}^+ \end{bmatrix} - M_r\right) \tag{24}$$

(j) Evaluate the effective tail-rotor collective pitch

$$\theta_{0T}^* = \frac{3}{1 + 3\mu_T^2/2}\left(\frac{2C_{T_T}}{a_{0_T} s_T} - \frac{\mu_{z_T} - \lambda_{0T}}{2}\right) \tag{25}$$

and the new tail-rotor collective pitch

$$\theta_{0_T}^+ = \theta_{0_T}^* \left[1 - k_3\gamma_T\left(1+\mu_T^2\right)/\left(8\lambda_{\beta_T}^2\right)\right] - k_3\gamma_T\left(\mu_{z_T} - \lambda_{0_T}\right)/\left(6\lambda_{\beta_T}^2\right) \tag{26}$$

(k) Stop the iteration if $\| \delta - \delta^+ \| \le \varepsilon$ is achieved; otherwise, reset $\delta = \delta^+$ and repeat the steps (b) ~(k).

5 Flight Simulation

Numerical simulation environment will be constructed for the validation of the nonlinear H_∞ control law designed earlier. The simulation flow chart is depicted in Fig.1. The following are the procedures for helicopter

(1) Evaluate β_0, β_{1c}, β_{1s}, λ_0 and λ_{0_T} according to the current state variables and control variables θ_0, θ_{1c}, θ_{1s}, and θ_{0_T}.

(2) Search for fuselage aerodynamic coefficients:
C_{x_f}, C_{y_f}, C_{z_f}, C_{l_f}, C_{m_f}, C_{n_f}, $C_{z_{tp}}$, $C_{y_{fin}}$.

(3) Compute aerodynamic forces and moments by the formulas.

(4) Substitute forces and moments into Eqs.(1) and integrate the resultants to obtain U, V, W, P, Q, and R.

(5) Use P, Q and R to compute quaternion by integration.

(6) Transform quaternion into Euler angles.

(7) Calculate the tracking errors of velocity, *u, v, w,* and body rate *p, q, r*.

(8) Feed *u, v, w, p, q, r* back to the nonlinear H_∞ controller to obtain the commanded forces and moments by employing Eq.(11) and Eq.(16).

(9) Determine C_T, β_{1s}, β_{1c} and C_{T_T} from Eq.(21), and determine pitch angles θ_0, $\theta_{1c_{hw}}$, $\theta_{1s_{hw}}$ from Eq.(24)

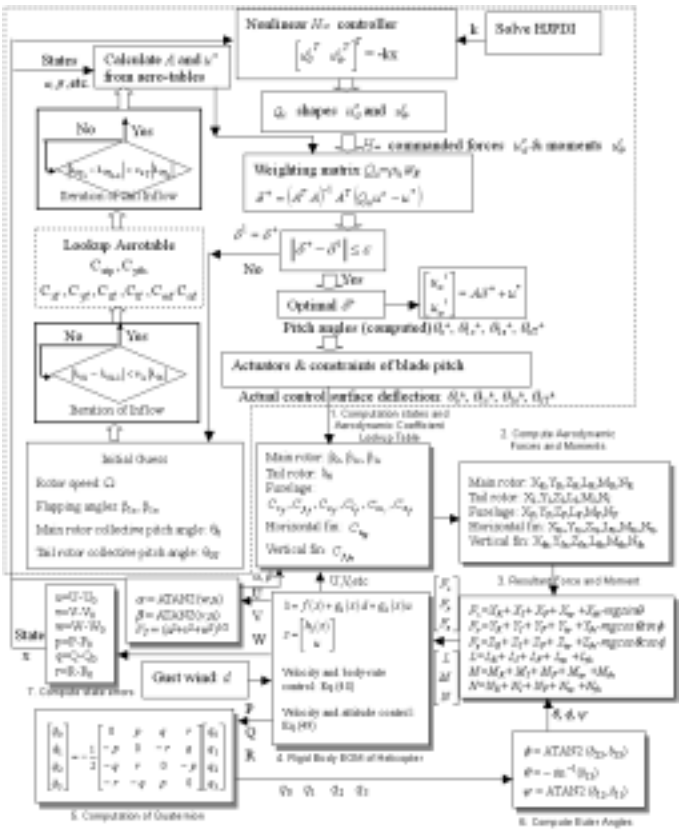

Fig.1 Flow chart for nonlinear H_∞ helicopter control.

5.1 Regulation of Nonlinear H_∞ Hovering Control

To illustrate that the convergence of the nonlinear H_∞ hovering control with actuator constraints is not merely local, we perturb the six DOF nonlinear motion to an initial condition far from trim condition, and then verify its convergence. The pitch control actuators are modeled as two cascade second order systems with damping ratio 0.7 and natural frequencies 140 and 70 for fly-by-wire and primary actuators, respectively, as shown in Fig.2. The main motor and tail rotor collective pitches are limited between [6.25^0 23.25^0]. The allowable intervals for longitudinal and lateral cyclic pitches are [-8.7^0 14^0] and [-7^0 8^0], respectively.

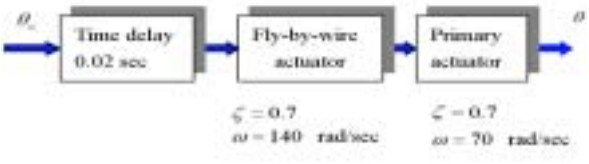

Fig.2 Actuator model

Initial perturbed condition: $\Sigma=[U\ V\ W]^T=[20\ 20\ 20]$ (m/sec), $\Omega=[P\ Q\ R]^T=[0.5\ .5\ 1]$ (rad/sec) and desired trim condition: $\Sigma_0=[U_0\ V_0\ W_0]^T=[0\ 0\ 0]$ (*m/sec*), $\Omega_0=[P_0\ Q_0\ R_0]^T=[0\ 0\ 0]$ (*rad/sec*).The upper bound of the L_2-gain is selected to $\gamma=2$; the weighting coefficients ρ_ε is set to 0.5, and the weighting Q_u is consisting of $Q_u=\rho_u W_E$.

$$\rho_u=\begin{bmatrix}0.01I_3 & 0\\ 0 & 0.12I_3\end{bmatrix},\quad W_E=\begin{bmatrix}4 & & & & & \\ & 1 & & & 0 & \\ & & 0.5 & & & \\ & & & .8 & & \\ & & 0 & & 0.03 & \\ & & & & & 1.5\end{bmatrix}$$

Substituting the above given data into Eq.(12) and Eq.(16) yields the admissible bounds for the feedback gains $C_\sigma=1.3978$ and $C_\omega=.8981$ which are, in turn, used in Eq.(11) and Eq.(16) to give the required control force u_σ and moment u_ω.

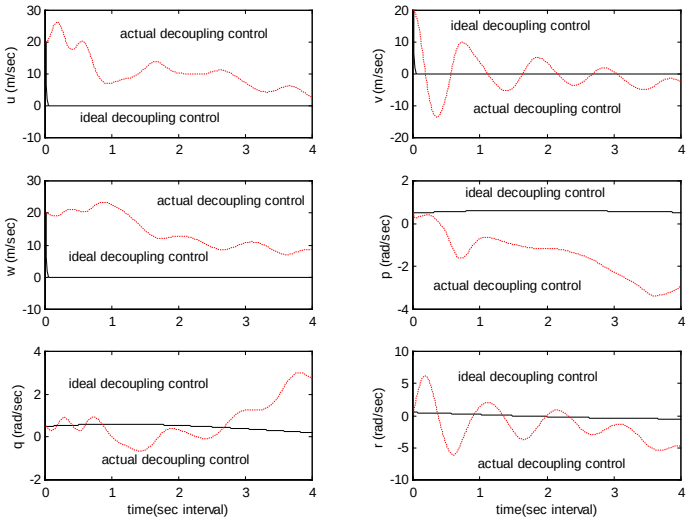

Figure 3 State responses of hovering control. Solid lines denote normal hovering control. Dashed lines denote variables θ_{1c} and θ_{0T} failing to work

The initial condition is very far from the equilibrium states. We plot the state responses in Fig.3 for control inputs of $u=u^a$. u^a is the control surface deflection commands (u^b) with both amplitude and rate constraints. The longitudinal states *u, w, q* converge at about 15 sec and downward speed *w* approaches the steady state about 2 m/sec, while the lateral states *v, p, r* converge rapidly at about 1.5 sec without steady state error. It reveals that the control ability in the longitudinal direction is not very well. The drawback can be overcome by adjusting the shaping and weighting matrix. Dashed lines in Fig 3 show the response when control variables θ_{1c} and θ_{0T} fail to work. We assume θ_{1c} and θ_{0T} are fastened at 0^0. Under this situation, convergent rate is very slow in forward speed deviation *u* and causes large steady-state error 10 m/sec in downward speed deviation *w*, while there are little effects in pitch rate deviation *q*. Without the control variables θ_{1c} and θ_{0T} defection, nonlinear H_∞ controller still has sufficient ability to stabilize the lateral states.

5.2 Verification of Decoupling Control in Hovering Mode

We have mentioned the property that under nonlinear H_∞ control structure, the hovering attitude control can be separated from the hovering velocity control. To illustrate the separation principle of the nonlinear H_∞ hovering control with/without actuator constraints, we perturb the six DOF nonlinear motion to an initial condition far from trim condition, and then verify its convergence.

As has been shown the hovering attitude control loop and the hovering velocity control loop for vertical take-off and landing vehicles can be designed independently under the framework of nonlinear H_∞ control. To verify this decoupling property numerically, we intentionally disconnect the hovering attitude controller, and let only nonlinear H_∞ velocity controller obtained from Eq.(16) remain operational. The trim condition for hovering mode is $\Sigma_0=\Omega_0=0$, and let the initial conditions for the perturbation be $[u(0)\ v(0)\ w(0)]=[100\ 100\ 100]$ (ft/sec) and $[p(0)\ q(0)\ r(0)]=[0.1\ 0.1\ 0.1]$ (rad/sec). The RMS time responses of the corresponding six DOF motion for $u=u^c$ case is plotted (solid line). As expected, the uncontrolled attitude loop is divergent, but the velocity loop is convergent under the nonlinear H_∞ control, being not influenced by the divergent attitude dynamics. For $u=u^a$ case, it is difficult for pitch blade deflections to create such control forces and moments that only control velocities but not for body rates. The fact can be observed in the linear control matrix *B* that all control variable deflections affect all velocities *u, v, w* and body rates *p, q, r*. Hence, we let control variable deflections θ_0, θ_{1s}, θ_{1c}, and θ_{0_T} only track control forces F_x, F_y, F_z, and disconnect the hovering attitude controller, hence only nonlinear H_∞ velocity controller remains operational. On the other hand, for the trim condition $\Sigma_0=\Omega_0=0$, the control surface matrix *A* can be calculated from Eq.(20) as follows

$$A=\begin{bmatrix}0.0676 & 0 & 0 & 0\\ -0.0043 & 0 & 0 & 0.03\\ 0.9977 & 0.0000 & -0.0000 & 0\\ 0 & -0.0001 & -0.0067 & 0.0054\\ -0.0107 & -0.0067 & 0.0001 & 0\\ -0.0000 & -0.0000 & -0.0005 & -0.0358\end{bmatrix}$$

One can find that forces are mainly produced by C_T and C_{T_T}, while β_{1c} and β_{1s} almost have no effect to them. Therefore, only C_T and C_{T_T} are chosen to track required forces. We assume that β_{1c} and β_{1s} are fixed at trim condition –0.008 and 0.0042, respectively. The ρ_u and W_E are set as following:

$$W_E = \begin{bmatrix} 0.5 & & & \\ & 1 & & 0 \\ & & 0.5 & \\ & & & \\ & 0 & & * \end{bmatrix}, \quad \rho_u = \begin{bmatrix} 0.01I_3 & 0 \\ 0 & * \end{bmatrix}$$

where the symbol * here denotes that we don't care the value. It is noticed that the control variable deflections $\theta_0, \theta_{1s}, \theta_{1c}$ are transformed from β_0, β_{1c}, β_{1s} in Eq.(24). It means that even β_{1c} and β_{1s} are fixed, θ_{1s} and θ_{1c} will not be constant.

The decoupling control verification for control input of $u=u^a$ case shows in Fig.4 where initial condition are $\Sigma=[U\ V\ W]^T=[20\ 20\ 20]$ (*m/sec*), and $\Omega=[P\ Q\ R]^T=[0.5\ 0.5\ 0.5]$ (*rad/sec*). This decoupling phenomenon can be observed from

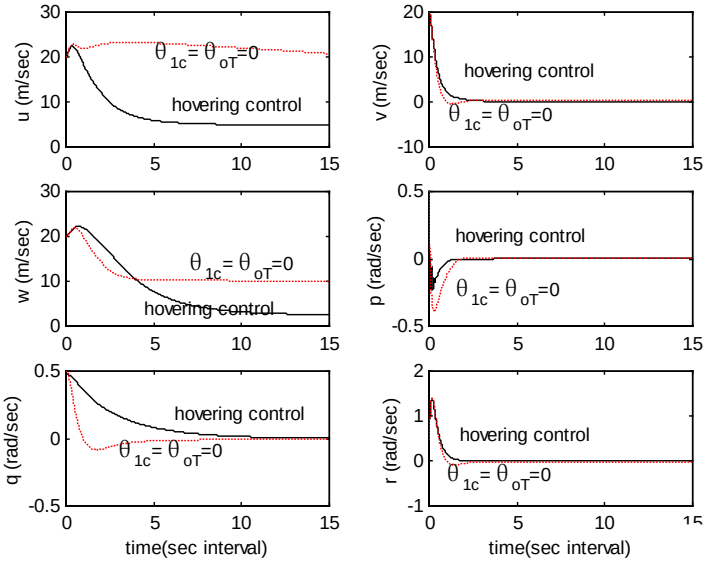

Figure 4 State responses with velocity controllers and without attitude controllers for $u=u^c$ and $u=u^a$ cases.

velocities are stabilized and body rates are divergent. It is noticed that the decoupling effect in nonlinear H_∞ hovering control has not the assumption of small perturbation. The initial condition is far from the equilibrium states. This decoupling property is different to linear flight control design wherein longitudinal control can be decoupled from lateral control when vehicle's perturbation is small, especially body rates.

While the separation principle is valid only during the 3 sec shown in Fig. 5. The induced forces from divergent body rates exceed the control forces created by control variable deflections. It can be realized that the control variable deflection θ_0, θ_{1s}, θ_{1c}, θ_{0T} are all saturated for t>3.5 sec. It implies that actuator restrains decoupling control ability. The decrease of Ω_Γ, which is dependent on the increase of θ_0. One can notice t>4.35 sec that the helicopter will tend to crash with a too low Ω_Γ because of the long time saturation of collective pitch. Another limitation of actuator to separation principle is the convergent rate. For $u=u^c$ case, velocities converge at about 0.15 sec and body rates remain around steady state condition, but there is slow convergent rate for $u=u^a$ case. However, the responses still show the tendency of separation property for nonlinear H_∞ hovering control.

6 Conclusions

In this paper helicopter hovering controllers were designed under the complete six degree-of-freedom equations of motion without the assumption of small perturbation. The key feature of this paper is the practical discussion on how to implement blade pitch angles from the nonlinear H_∞ command. Regulation and separation principle of nonlinear H_∞ hovering control were validated via control surface inverse algorithm (CSIA). The separation principle is valid no more than actuators being working. In ideal case, if actuators could output arbitrarily, the separation principle of nonlinear $H\infty$ hovering control would be always valid.

References

[1] Padfield, G. D., *Helicopter Flight Dynamics: The Theory and Application of Flying Qualities and Simulation Modeling*, AIAA, (1996).

[2] Apkarian, P. et al "Design of a helicopter output feedback control law using modal and structured -robustness technique," *Journal of Control*, **V. 50**, (1989).

[3] Kang, W., "Nonlinear H_∞ Control and Its Applications to Rigid Spacecraft," *IEEE Transactions on Automatic Control*, **Vol.40**, pp.1281-1285, (1995).

[4] Yang, C. D. and Kung, C. C., "Nonlinear H_∞ Flight Control of General Six Degree-of-Freedom Motions," *AIAA Journal of Guidance Control, and Dynamics,* **Vol.23, No. 2**, pp. 278-288, (2000).

[5] Van der Schaft, A. J., "L_2-gain Analysis of Nonlinear Systems and Nonlinear H_∞ Control," *IEEE Transactions on Automatic Control*, **Vol. 37**, pp. 770-784, (1992).

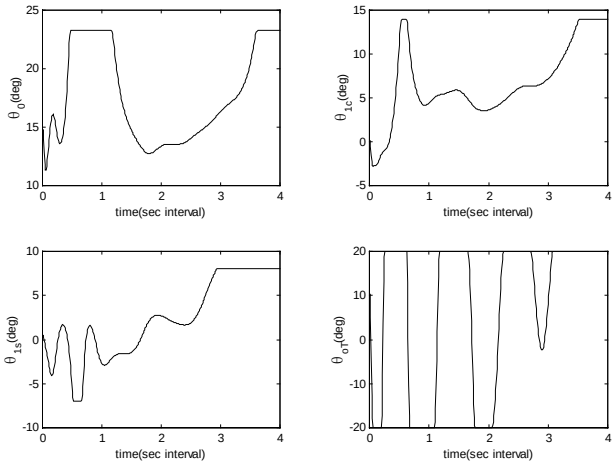

Figure 5 Histories of control variable deflections with velocity controllers and without attitude controllers for $u=u^a$ case.